



CASE REPORT

Orbital rhabdomyosarcoma and traumatic neuroma following enucleation for a uveal schwannoma in a dog: a case report

Jessica E. McDonald¹ , Amy M. Knollinger¹, Leandro B. Teixeira²  & Richard R. Dubielzig²

¹Eye Care for Animals, 1021 E. 3300 S., Salt Lake City, Utah 84106, USA

²Comparative Ocular Pathology Laboratory of Wisconsin, School of Veterinary Medicine, University of Wisconsin-Madison, 2015 Linden Drive, Madison, Wisconsin 53706, USA

Correspondence

Jessica E. McDonald, Eye Care for Animals, 1021 E. 3300 S., Salt Lake City, UT 84106, USA. Tel: 801-942-3937; Fax: 801-942-4302; E-mail: jmcdonald@eyecareforanimals.com

Funding Information

No sources of funding were declared for this study.

Received: 28 September 2016; Revised: 20 December 2016; Accepted: 8 January 2017

Clinical Case Reports 2017; 5(3): 300–307

doi: 10.1002/ccr3.842

Introduction

Uveal schwannomas, previously known as spindle cell tumor of blue-eyed dogs (SCTBED), were first described by Zarfoss et al. in 2007 [1]. These tumors develop in the anterior uvea of dogs with blue iridal tissue; however, limited literature is available with [2] one case report of uveal schwannoma exists occurring in the anterior uvea in a cat [3]. Uveal schwannomas are comprised of two cell patterns: spindle cells with nuclei arranged in stacked alignments, or palisades (an Antoni-A pattern) and spindle cells arranged in interlacing bundles and sheets (an Antoni-B pattern) that are vimentin and S100 positive, indicating mesenchymal and neural crest origins. In addition, glial fibrillary acidic protein (GFAP) marker is commonly positive in these tumors, suggestive of central nervous system origin [1, 3]. Biologic behavior of these tumors is unclear and although generally considered benign, malignancy is described in a Beagle [3], Labrador retriever [4], and a mixed breed dog [5]. Although Siberian Huskies are over-represented for the presence of uveal schwannoma within the

Key Clinical Message

A 4-year-old, female spayed Siberian husky with history of a uveal schwannoma presented for orbital swelling 9 months after enucleation. A second, malignant tumor developed in the same orbit. Therefore, uveal schwannomas may warrant early surgical intervention in the dog.

Keywords

Canine, enucleation, orbit, rhabdomyosarcoma, schwannoma, traumatic neuroma.

Comparative Ocular Pathology Laboratory of Wisconsin (COPLOW) database, no reports of malignancy have been reported in this breed thus far.

Rhabdomyosarcomas are soft tissue mesenchymal neoplasms rarely reported in the orbit of dogs [6, 7]. In humans, rhabdomyosarcomas are rare in adults, but comprise of >50% of all soft tissue sarcomas in children [8–10], and are classified into embryonal, alveolar, and pleomorphic types in both species [11, 12]. Similar to the age distribution in humans, canine rhabdomyosarcomas typically occur in animals <2 years of age [6].

The purpose of this report was to describe an orbital rhabdomyosarcoma that occurred 9 months after enucleation and placement of an intraorbital prosthesis for uveal schwannoma in a Siberian husky. We propose that the chronicity of the uveal schwannoma prior to enucleation and the inflammation or aberrant wound healing induced to the orbital tissues by this tumor may have predisposed subsequent orbital rhabdomyosarcoma development. Therefore, early surgical intervention may be warranted for uveal schwannomas in dogs.

Case Report

History and clinical signs

A 4-year-old female spayed Siberian husky was presented to an ophthalmology specialty clinic with a two-week history of redness and mild blepharospasm of the right eye (OD) that had become progressively worse prior to presentation.

On ophthalmic examination, the patient was visual including positive menace response in both eyes (OU). Dazzle reflex was also positive OU, as well as positive direct and consensual pupillary light reflexes OU. Slit lamp biomicroscopy (SL-14, Kowa, Ltd., Tokyo, Japan) revealed rubeosis iridis and an irregular pupillary margin were observed toward the temporal aspect of the iris from the 7 o'clock to 12 o'clock position OD. Decreased intraocular pressure (IOP) was 5 mmHg via rebound tonometry OD versus 12 mmHg in the left eye (OS) (TonoVet[®], Icare Finland Oy, Helsinki, Finland). Schirmer tear test-1 was within normal limits at 28 mm/min OU, and fluorescein uptake was negative OU. Stable iris-to-iris persistent pupillary membranes (PPMs) were observed OU throughout all exams. Fundic examination OD was within normal limits via indirect ophthalmoscopy (Keeler Fison Binocular Indirect Ophthalmoscope, Keeler Instruments Inc., Broomall, PA). Ophthalmic and fundic examination OS, other than the previously noted PPMs, was within normal limits throughout all exams. Due to the diagnosis of anterior uveitis, systemic bloodwork, thoracic radiographs, and infectious disease testing were recommended; however, all were declined. Diclofenac 0.1% (Akorn[®] Inc., Lake Forest, IL) was initiated OD BID and artificial tear ointment (Rugby[®] Laboratories, Livonia, MI) OU BID. Recheck examination was recommended in 2–3 weeks.

Three months later, the patient was re-presented with recurrent signs of uveitis OD. The patient had been treated with 0.1% diclofenac OU BID and artificial tear ointment OU BID since previous examination. The patient was visual OU. Ophthalmic examination, however, revealed thickening of the iris with irregular pupillary margin and rubeosis iridis in the same temporal region OD as previously described. Mild aqueous flare was noted in the anterior chamber OD. In addition, an iridociliary cyst was also noted through the pupillary aperture arising from the posterior iris epithelium from the 9 o'clock to 11 o'clock position OD. Intraocular pressure (IOP) measured 9 mmHg OD and 25 mmHg OS via rebound tonometry. Schirmer tear test-1 was within normal limits OU, and fluorescein uptake was negative OU. Diclofenac and artificial tear ointment were discontinued, and 1% prednisolone acetate (Alcon[®], Fort Worth, TX) OD TID

was initiated due to continued evidence of anterior uveitis. Recheck examination was recommended in 2 weeks.

One month later, or 4 months after initial presentation, progressive thickening of the iris and rubeosis iridis OD was noted from the 7 o'clock to 3 o'clock position OD (Fig. 1). No evidence of aqueous flare was noted OD. Pupillary margin irregularity was present at this time from the 7 o'clock to 5 o'clock position OD. Intraocular pressure (IOP) had increased from 12 mmHg at previous examination to 15 mmHg via rebound tonometry. Fluorescein uptake was negative OU. No changes in medical therapy were performed at this time, however, enucleation was recommended due to progression of disease and concern for intraocular neoplasia OD. Differentials for the thickening OD included the following neoplasms: uveal schwannoma, iridociliary adenoma/carcinoma, lymphoma, histiocytic sarcoma, and amelanotic melanoma. Anterior uveitis secondary to infectious causes including tick-borne, protozoal, and idiopathic etiologies was also considered based on the patient's unilateral presentation and lifestyle. Prednisolone acetate 1% was continued OD TID.

Three months later, or 7 months after initial presentation, the patient remained visual OU, including positive menace response. Dazzle reflexes were also positive OU. The thickening of the iris OD had not progressed, and no aqueous flare was noted OD; however, an additional iridociliary cyst was present arising from the posterior iris at the 2 o'clock to 3 o'clock position OD. Intraocular pressures were elevated OD to 24 and 12 mmHg OS. Fluorescein uptake was negative OU. Enucleation was recommended at this time due to progression of IOP OD. Latanoprost 0.005% ophthalmic (Bausch and Lomb[™], Bridgewater, NJ) was initiated OD BID, and



Figure 1. Clinical photograph of a 4-year-old female, spayed Siberian husky. Thickening of the iris was prominent with pupillary margin irregularity and rubeosis iridis in the temporal region OD from 7 o'clock to 3 o'clock hours.

prednisolone acetate was continued as previously prescribed until surgery could be pursued.

Systemic bloodwork, including complete blood count, serum chemistry, and urinalysis, was performed prior to enucleation OD to ensure the patient was systemically healthy prior to general anesthesia. The only abnormality noted was an elevated urine pH [9.0 (5.5–7.0)], as well as trace proteinuria, and the remainder was within normal limits. Thoracic radiography and abdominal ultrasound were performed and revealed no gross abnormalities per review by a board-certified radiologist. A transconjunctival enucleation OD was performed 2 weeks after the last recheck ophthalmic examination, or 8 months after initial presentation, in a standard manner, and a 20-mm black intraorbital prosthetic (Acri.Orbit Silicone Prosthesis, Acrivet Inc., Salt Lake City, UT) was placed. The orbital rim and subcutaneous tissues, individually, were sutured with 4-0 polyglactin 910 (Vicryl[®], Ethicon, NJ) in a simple continuous pattern, and the skin was sutured with 4-0 polypropylene (Prolene[®], Ethicon, NJ) in a simple interrupted pattern. Cephalexin (Alkem Laboratories, Ltd., NJ [27.0 mg/kg (12.2 mg/lb) PO BID] for 14 days and

tramadol (Amneal Pharmaceuticals, KY [2.7 mg/kg (1.22 mg/lb) PO BID] for 7 days were initiated.

The globe was submitted to the Comparative Ocular Pathology Laboratory of Wisconsin (COPLOW) for histopathological analysis, which confirmed a dense population of neoplastic spindle cells arranged in interlacing bundles and sheets (an Antoni-B pattern) infiltrating and distorting the iris leaflets and ciliary body (Fig. 2A and B). The population of cells were monomorphic and small and occluded the ciliary cleft and iridocorneal angle (ICA). The posterior pigmented iridal epithelium extended over the anterior surface of the iris at the pupillary margin, causing the clinical appearance of the irregular pupillary margin. Glial fibrillary acid protein (GFAP) immunohistochemistry staining was performed and found to be regionally positive (Fig. 2C). Therefore, a diagnosis of uveal schwannoma was confirmed and histopathology confirmed clean surgical margins. The patient healed without complication following enucleation, and sutures were removed 2 weeks after surgery.

Nine months after surgery, or 1.4 years after initial presentation, the patient was re-presented for a 2-week

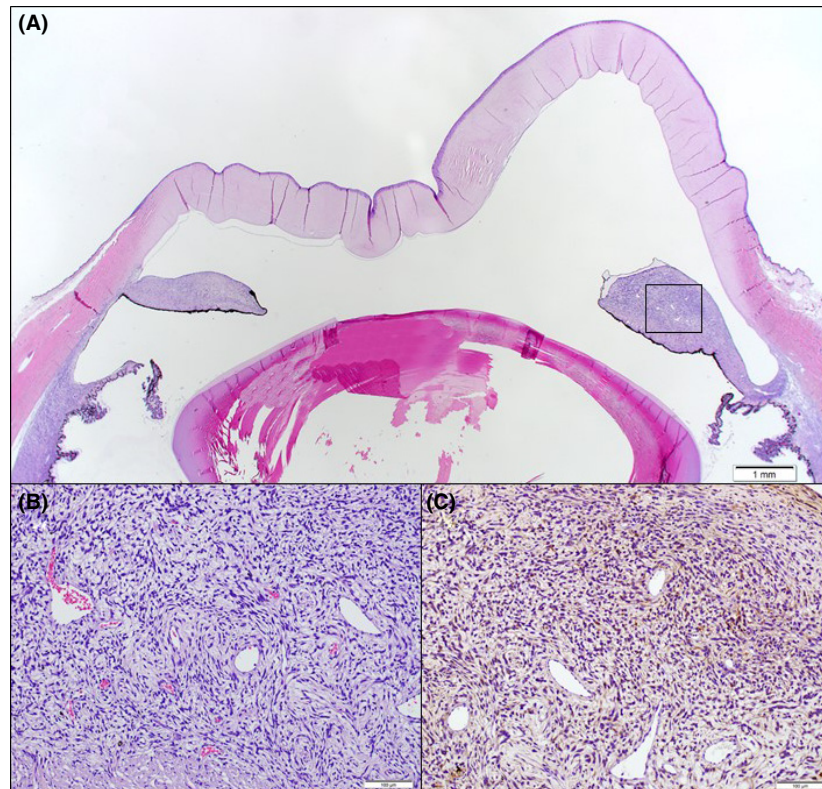


Figure 2. Histopathology OD, schwannoma of blue-eyed dogs. (A) Subgross image revealing a basophilic mass expanding and distorting the iris leaflets, ciliary body, and iridocorneal angle. H&E. Bar = 1 mm (B) Photomicrograph, inset from (A), showing fusiform neoplastic cells with scant cytoplasm, forming variably dense, short interlacing bundles. H&E. Bar = 100 μ m. (C) Photomicrograph showing varying degrees of positive cytoplasmic staining for GFAP. Bar = 100 μ m.



Figure 3. Clinical photograph under general anesthesia prior to MRI of a firm orbital swelling noted 9 months after the enucleation for a uveal schwannoma OD, or 3 years 5 months after initial presentation. Diffuse hyperemia and pain were noted during examination of this region.

history pain around the healed incision. On palpation, a firm swelling was noted within the right orbit (Fig. 3). Thoracic radiographs and magnetic resonance imaging (MRI) were recommended to determine the extent of the mass and potential of metastatic disease. Three-view thoracic radiographs were performed and were free of gross visible disease per board-certified radiologist review. Magnetic resonance imaging (MRI) T2-weighted postcontrast sequences revealed a hyperintense soft tissue mass along

the rostral and medial aspect of the right orbit, causing displacement of the orbital prosthesis uniformly anteriorly (Fig. 4). The mass was contrast-enhancing and distorted the medial margin of the orbit with no definitive changes observed with the musculature in the caudal aspect of the orbit. An incisional punch biopsy of the mass was performed after MRI, which was submitted to the Colorado State University Veterinary Diagnostic Laboratory for histopathological analysis. Histopathology revealed a grade 3 undifferentiated sarcoma, which consisted of spindle cells that formed whorls with interweaving bundles. Nucleoli were prominent with 3–5 mitotic figures per 100x high-powered field.

After diagnosing the undifferentiated sarcoma, consultation to a board-certified radiation oncologist including potential exenteration and radiation therapy at Colorado State University was offered, but was declined by the owner.

Four weeks after diagnosing the orbital sarcoma, the patient presented for exenteration for palliative purposes at the referring veterinarian. The orbital tissues were obtained by the ophthalmology specialty clinic and were submitted for histopathological analysis to COPLOW. Grossly, the orbital prosthesis was surrounded by a thick fibrous capsule that was not penetrated by the surrounding neoplastic tissue. Histologically, the superficial and deep dermis, subcutaneous tissues, and orbital connective tissue were infiltrated and partially replaced by poorly delineated, nonencapsulated neoplastic mass (Fig. 5A and B). This mass was composed of fusiform to epithelioid cells arranged in solid sheets and presenting marked cellular pleomorphism with multinucleated and karyomegalic

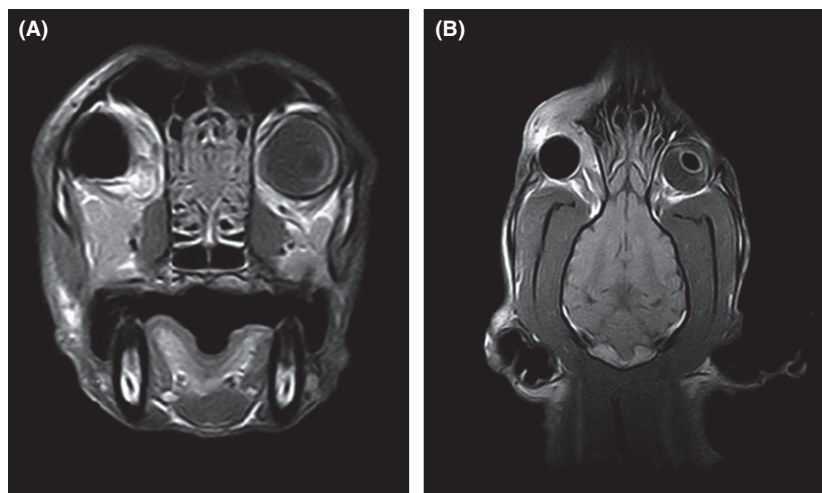


Figure 4. (A) Axial T1-weighted and (B) dorsal T1-weighted postcontrast MRI images. Note the lobular mass, representing an orbital mass, rostral and medial to the right prosthetic causing uniform anterior displacement of the intraorbital prosthesis. The postcontrast image highlights perilesional heterogenous tissue enhancement. No definitive changes were observed with the musculature in the caudal aspect of the orbit.

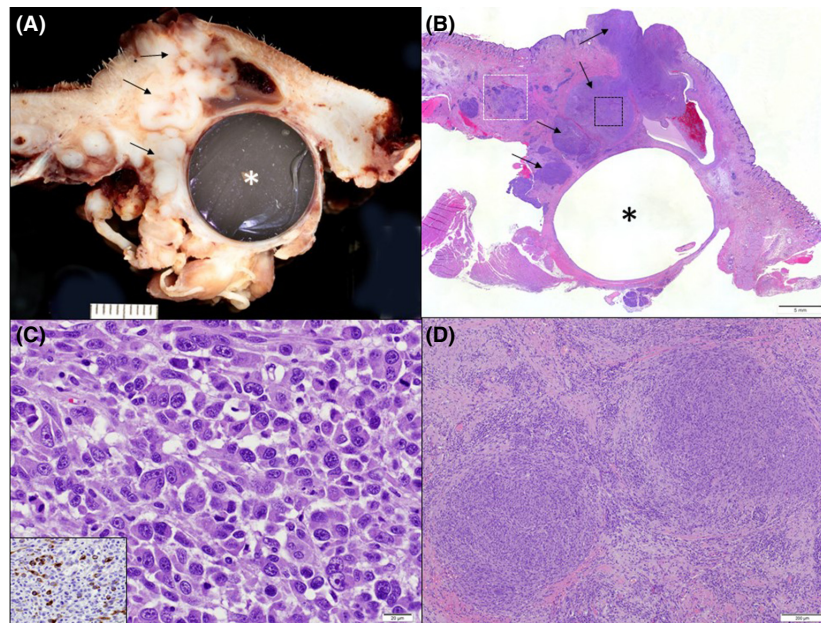


Figure 5. Histopathology exenteration and intraorbital prosthesis, rhabdomyosarcoma. (A) Gross imaging of the formalin-fixed tissue presenting the intraorbital prosthesis (*) surrounded by a firm, tan, multilobulated mass (arrows). (B) Subgross image revealing a dense, multilobular neoplastic mass infiltrating and expanding the superficial and deep dermis, subcutaneous and orbital connective tissue (arrows) around the orbital prosthesis (*) that was removed for histologic processing. H&E. Bar = 5 mm. (C) Photomicrograph, inset from black box in (A), showing rafts of highly pleomorphic and haphazardly arranged polygonal cells with moderate amounts of eosinophilic cytoplasm and highly pleomorphic nuclei. H&E. Bar = 20 μ m. Inset: Photomicrograph showing varying degrees of positive cytoplasmic immunohistochemical staining for desmin. (D) Photomicrograph, inset from white box in (A) showing two distinct masses composed of proliferating redundant fusiform cells adjacent to large peripheral nerves, interpreted as traumatic neuromas. H&E. Bar = 200 μ m.

cells and an average of 7.3 mitotic figures per single high-powered field (Fig. 5C). Immunohistochemistry revealed negative markers for GFAP and skeletal muscle actin and a positive marker for desmin, consistent with the diagnosis of rhabdomyosarcoma. In addition to the mass, there were three distinct other masses away from the body of the rhabdomyosarcoma composed of proliferating redundant fusiform cells that surrounded or were adjacent to large peripheral nerves, consistent with traumatic neuromas (Fig. 5B and D). Severe lymphoplasmacytic inflammatory infiltrate was found throughout the superficial dermis and orbital connective tissues encompassing all areas of rhabdomyosarcoma and traumatic neuromas.

Two weeks after exenteration, the orbital incision had dehisced and the referring veterinarian performed wet-to-dry bandaging for the open wound and recommended ophthalmic examination which was performed 4 weeks after exenteration. Examination was unremarkable OS. On ophthalmic examination, the incision had dehisced with exposed subcutaneous tissues underlying the previous incision site OD. Therefore, revision of the previous incision site was elected by the owner. The patient was anesthetized, the upper and lower eyelid margins were trimmed with Metzenbaum scissors, and the underlying

subcutaneous tissues were undermined with a 15 scalpel blade. The subcutaneous tissues were apposed with 4-0 polyglactin 910 (Vicryl[®], Ethicon, NJ) in a simple continuous pattern, and the skin was closed with 4-0 polypropylene (Prolene[®], Ethicon, NJ) in a horizontal mattress pattern. Following this examination, the patient was not re-presented to the ophthalmology specialty clinic. The patient was euthanized 6 weeks after exenteration due to worsening of systemic disease, including anorexia and lethargy. Per the referring veterinarian at the time of euthanasia, the surgical site had healed with no signs of dehiscence. No necropsy was performed after euthanasia.

Discussion

This case report describes a unique case of the development of two rare and seemingly unrelated neoplasms in the right globe, uveal schwannoma, and postoperatively in the right orbit, rhabdomyosarcoma, in a 4-year-old Siberian husky. This sequence of presentation of these neoplasms provokes an interesting discussion to potential biologic behavior and pathogenesis of the uveal schwannoma, although the etiology of uveal schwannoma is still

unclear. The behavior of this tumor is unclear at this time; however, they have been infrequently reported to be metastatic [3, 4]. In this case, scleral invasion of the uveal schwannoma was not found on initial histopathology OD, consistent with pathological findings of Duke *et al.* reporting that only 6/52 cases of uveal schwannoma in the COPLOW collection having scleral invasion [3]. Therefore, we hypothesize that aberrant wound healing or inflammation from the uveal schwannoma, rather than direct extension of schwannoma, induced the subsequent orbital rhabdomyosarcoma within this canine patient. Due to this hypothesis, the authors suggest that early surgical intervention, particularly enucleation, should be performed early in the course of the disease if a uveal schwannoma is suspected.

According to Grosopf *et al.*, soft tissue repair following enucleation in all species has three general steps: inflammation with resorption of necrotic tissue or exudates, proliferation of granulation tissue, and a maturation of granulation tissues with fibrosis. Typically, during the proliferative phase of tissue repair, cell-to-cell contact inhibition halts additional proliferation and aberrant cell growth once the repair phase is complete. It has been hypothesized that sarcomas can arise from wound healing when there are gene mutations of the proliferating cells due to rapid duplication; however, this process remains uncertain [13–16]. Several authors have reported chronic inflammation as suspected pathogenesis for many feline neoplasms, including extraskelatal osteosarcoma following enucleation in a cat [13], as well as feline injection-site sarcomas following long-acting antibiotics, anti-inflammatories, chemotherapy agents [17–20], and nonabsorbable suture material [21]. Microchip implants have also been implicated in fibrosarcoma formation in the cat [22, 23], and dog [24], as well as several mesenchymal neoplasms in the rat, including malignant schwannoma, fibrosarcoma, anaplastic sarcoma, and histiocytic sarcoma [25]. Orbital rhabdomyosarcomas have been reported in humans following blunt traumatic injury to the eyebrow in an adult [26], suspected to be due to aberrant skeletal muscle regeneration (SMR) after injury or inflammation. SMR has also been reported to histologically stimulate cutaneous malignancies such as squamous cell carcinoma and rhabdomyosarcoma in humans [27–29].

Although intraorbital prostheses are commonly used without complication, it cannot be ruled out that inflammation from the surgical removal of the uveal schwannoma, intraorbital prosthesis, or absorbable suture material used in the enucleation additively or solely provided the inciting skeletal inflammation to induce an orbital rhabdomyosarcoma. To the authors' knowledge, orbital implants and absorbable suture inducing tumorigenesis have not been reported in either the human or

veterinary literature to date. In cats with injection-site sarcomas, the latency period from the time of injection or onset of inflammation to tumor development in cats has been variedly reported from as short as 3 months to 3–10 years. In this case, the orbital rhabdomyosarcoma developed 9 months after enucleation, which is consistent with previously reported mesenchymal tumors [30, 31].

Another interesting finding within this case report is the presence of three traumatic neuromas in the exenteration sample submitted. Traumatic neuroma is a reactive lesion of neural origin that develops in a nerve bundle after trauma, such as an enucleation. During the repair process, axons grow to attempt to reestablish neural connections, sometimes proliferating into a mass resembling a reactive, excessive proliferative lesion at the site of injury. The potential for a reactive neuroma to initiate tumorigenesis through inflammation in this case cannot be excluded. However, the authors feel this is a low risk as reports of tumorigenesis coinciding with traumatic neuroma have not been reported in human literature.

Microscopically, the hallmark of traumatic neuroma is a haphazard arrangement of regenerating axons in a background of Schwann cells, perineural cells, and connective tissue elements [32]. Orbital traumatic neuromas have been previously diagnosed in humans after orbital decompression surgery; however, the majority of traumatic neuromas are a complication of orthopedic procedures [33, 34]. Traumatic neuromas are histologically somewhat similar in appearance to schwannomas but are more highly differentiated. These well-delineated neuromas were at the periphery of the main mass and composed of well-differentiated fusiform cells with distinct basement membrane. Along with the history of a previous enucleation, these histopathological findings supported the diagnosis of a traumatic neuroma rather than a schwannoma regrowth.

In this case, our first clinical interpretation was that the orbital neoplasm was a metastasis of the uveal schwannoma; however, this was diagnosed as a separate orbital rhabdomyosarcoma neoplasm based on histopathology and immunohistochemistry. Although they were in close proximity in location and time to each other, these two neoplasms are of separate pathogenesis, although the pathogenesis of schwannoma is not completely understood at this time. Therefore, this case lends evidence to a potential link between canine orbital sarcomas and unique inflammatory response similar to that in felines [13, 15–20]. Potential sources of inflammation, including the potential role of chronic irritation from the uveal schwannoma, causing rare highly aggressive secondary orbital neoplasia in dogs should be investigated. The etiology of the subsequent rhabdomyosarcoma in this case

cannot be elucidated at this time; however, based on this report, the authors suggest that early surgical intervention of uveal schwannomas is warranted.

Authorship

JEM: Primary clinical case responsibility; Primary author. AMK: Primary clinical case responsibility; Editor. LBT: Oculopathologist with Comparative Ocular Pathology Laboratory of Wisconsin (COPLOW); Editor. RRD: Oculopathologist with Comparative Ocular Pathology Laboratory of Wisconsin (COPLOW); Editor.

Conflict of Interest

None declared.

References

- Zarfoss, M. K., G. Klauss, K. Newkirk, M. Kiupel, Y. Jones, C. M. H. Colitz, et al. 2007. Uveal spindle cell tumor of blue-eyed dogs: an immunohistochemical study. *Vet. Pathol.* 44:276–284.
- Evans, P. M., G. L. Lynch, and R. R. Dubielzig. 2010. Anterior uveal spindle cell tumor in a cat. *Vet. Ophthalmol.* 13:387–390.
- Duke, F. D., D. K. Brudenall, E. M. Scott, L. B. C. Teixeira, and R. R. Dubielzig. 2013. Metastatic uveal schwannoma of blue-eyed dogs. *Vet. Ophthalmol.* 16:141–144.
- Duke, F. D., L. B. C. Teixeira, L. E. Galle, N. Green, and R. R. Dubielzig. 2015. Malignant uveal schwannoma with peripheral nerve extension in a 12-week-old color-dilute labrador retriever. *Vet. Pathol.* 52:181–185.
- Olbertz, L., I. Langohr, J. Werner, L. Pessoa, M. Kiupel, D. Agnew, et al. 2013. Anterior uveal spindle cell tumor in a blue-eyed mixed-breed dog. *Vet. Ophthalmol.* 16:135–140.
- Meunier, V., A. Fontaine, S. Leconte, F. Delisle, and I. Raymond-Letron. 2010. Exophtalmie et rhabdomyosarcome orbitaire chez un chien. *Prat. Med. Chir. Anim. Comp.* 45:101–106.
- Kato, Y., H. Notake, J. Kimura, M. Murakami, A. Hirata, H. Sakai, et al. 2012. Orbital embryonal rhabdomyosarcoma with metastasis in a young dog. *J. Comp. Pathol.* 147:191–194.
- Andrassy, R. J. 2002. Advances in the surgical management of sarcomas in children. *Am. J. Surg.* 184:484–491.
- Rehúrek, J., and R. Autrata. 1997. Clinical diagnosis of orbital rhabdomyosarcoma in a child. *Cesk. Slov. Oftalmol.* 53:215.
- Chen, S.-C., Y.-S. Bee, M.-C. Lin, and S.-J. Sheu. 2011. Extensive alveolar-type paranasal sinus and orbit rhabdomyosarcoma with intracranial invasion treated successfully. *J. Chin. Med. Assoc.* 74:140–143.
- Maxie, M. G., K. V. F. Jubb, P. C. Kennedy, and N. Palmer. 2007. Volume 1, Neoplastic Diseases of Muscle. Pp. 272–277 in M. Grant Maxie, ed. Jubb, Kennedy, and Palmer's pathology of domestic animals. 5th ed. Elsevier Saunders, Edinburgh, New York.
- Meuten, D. J., and J. E. Moulton. 2002. Chapter 6, Tumors of Muscle. Pp. 319–363 Tumors in domestic animals, 4th ed. Iowa State University Press, Ames, Iowa.
- Groskopf, B. S., R. R. Dubielzig, and S. L. Beaumont. 2010. Orbital extraskeletal osteosarcoma following enucleation in a cat: a case report. *Vet. Ophthalmol.* 13:179–183.
- Haran-Ghera, N., N. Trainin, L. Fiore-Donati, and I. Berenblum. 1962. A possible two-stage mechanism in rhabdomyosarcoma induction in rats. *Br. J. Cancer* 16:653.
- Hershey, A. E., R. R. Dubielzig, M. L. Padilla, and S. C. Helfand. 2005. Aberrant p53 expression in feline vaccine-associated sarcomas and correlation with prognosis. *Vet. Pathol.* 42:805–811.
- Sappino, A. P., and W. Schurch. 1990. Gabbiani: differentiation repertoire of fibroblastic cells: expression of cytoskeletal proteins as marker of phenotypic modulations. *Lab. Invest.* 63:144–161.
- Kass, P. H., W. L. Spangler, M. J. Hendrick, L. D. McGill, G. Esplin, S. Lester, et al. 2003. Multicenter case-control study of risk factors associated with development of vaccine-associated sarcomas in cats. *J. Am. Vet. Med. Assoc.* 1:1283–1292.
- Martano, M., E. Morello, and P. Buracco. 2011. Feline injection-site sarcoma: past, present and future perspectives. *Vet. J.* 188:136–141.
- Munday, J. S., K. Banyay, D. Aberdein, and A. F. French. 2011. Development of an injection site sarcoma shortly after meloxicam injection in an unvaccinated cat. *J. Feline Med. Surg.* 13:988.
- Martano, M., E. Morello, S. Iussich, and P. Buracco. 2012. A case of feline injection-site sarcoma at the site of cisplatin injections. *J. Feline Med. Surg.* 14:751–754.
- Buracco, P., M. Martano, E. Morello, and A. Ratto. 2002. Vaccine-associated-like Fibrosarcoma at the Site of a Deep Nonabsorbable Suture in a Cat. *Vet. J.* 163:105–107.
- Daly, M. K., C. F. Saba, S. S. Crochik, E. W. Howerth, C. E. Kosarek, K. K. Cornell, et al. 2008. Fibrosarcoma adjacent to the site of microchip implantation in a cat. *J. Feline Med. Surg.* 10:202–205.
- Carminato, A., M. Vascellari, W. Marchioro, E. Melchiotti, and F. Mutinelli. 2011. Microchip-associated fibrosarcoma in a cat. *Vet. Dermatol.* 22:565–569.
- Vascellari, M., E. Melchiotti, and F. Mutinelli. 2006. Fibrosarcoma with typical features of postinjection sarcoma at site of microchip implant in a dog: histologic and immunohistochemical study. *Vet. Pathol.* 43:545.
- Elcock, L. E., B. P. Stuart, B. S. Wahle, H. E. Hoss, K. Crabb, D. M. Millard, et al. 2001. Tumors in long-term

- rat studies associated with microchip animal identification devices. *Exp. Toxicol. Pathol.* 52:483–491.
26. Bagdonaite, L., I. Jeeva, B. Y. P. Chang, G. Kalantzis, and N. El-Hindy. 2013. Multidisciplinary management of adult orbital rhabdomyosarcoma. *Orbit* 32:208.
 27. Ghosn, S. H., A. Radfar, and C. M. Stefanato. 2007. Skeletal muscle regeneration: report of a case presenting as a cutaneous nodule following blunt trauma to the lip. *J. Cutan. Pathol.* 34:352–354.
 28. Stefanato, C., M. Mahalingam, S. Kates, and J. Bhawan. 2003. Skeletal muscle regeneration: report of a case simulating squamous cell carcinoma. *G. Ital. Dermatol. Venereol.* 138:41–45.
 29. Guillou, L., M. Coquet, P. Chaubert, and J. M. Coindre. 1998. Skeletal muscle regeneration mimicking rhabdomyosarcoma: a potential diagnostic pitfall. *Histopathology* 33:136–144.
 30. Séguin, B. 2002. Injection site sarcomas in cats. *Clin. Tech. Small Anim. Pract.* 17:168–173.
 31. McEntee, M. C., and R. L. Page. 2001. Feline vaccine-associated sarcomas. *J. Vet. Intern. Med.* 15:176.
 32. Silami, M. A. N. C., D. R. Camisasca, M. D. Sother, R. De Souza Azevedo, and S. P. De Oliveira. 2014. Traumatic neuroma: report of two cases. *Oral Surg. Oral Med. Oral Pathol. Oral Radiol.* 117:e193.
 33. Patel, S. S., B. J. Lee, and V. M. Elner. 2012. Painful traumatic neuroma after orbital decompression surgery. *Arch. Ophthalmol.* 130:530.
 34. Park, C.-H., D. Kojima, H. Hatai, S. Inoue, and T. Oyamada. 2012. A Case report of traumatic neuroma of the cervical spinal cord in a dog. *J. Vet. Med. Sci.* 74: 787–790.